Journal of Hazardous Materials 192 (2011) 949–955

Contents lists available at ScienceDirect

Journal of Hazardous Materials

journal homepage: www.elsevier.com/locate/jhazmat

Novel Cu (II) magnetic ion imprinted materials prepared by surface imprinted technique combined with a sol–gel process

Xubiao Luo[a,b], Shenglian Luo[a,b,*], Youcai Zhan[a,b], Hongying Shu[a,b], Yining Huang[a,b], Xinman Tu[a,b]

[a] Key Laboratory of Jiangxi Province for Ecological Diagnosis-Remediation and Pollution Control, Nanchang 330063, PR China
[b] College of Environmental and Chemical Engineering, Nanchang Hangkong University, Nanchang 330063, PR China

ARTICLE INFO

Article history:
Received 28 November 2010
Received in revised form 11 May 2011
Accepted 13 May 2011
Available online 7 July 2011

Keywords:
Cu (II)
Magnetic ion imprinted polymer
Surface imprinted technique
Sol–gel process

ABSTRACT

A novel Cu (II) magnetic ion-imprinted polymer (MIIP) was synthesized by surface imprinting technique combined with a sol–gel process. The adsorbent of Cu (II)-MIIP shows higher capacity and selectivity than that of magnetic non-imprinted polymers (MNIP). Adsorption capacities of Cu (II)-MIIP and MNIP are 24.2 and 5.2 mg/g for Cu (II) ions, respectively. The selectivity coefficients of the Cu (II)-MIIP for Cu (II)/Zn (II) and Cu (II)/Ni (II) are 91.84 and 133.92, respectively. Kinetics studies show that the adsorption process obeys pseudo-second-order rate mechanism with an initial adsorption rate of 132.48 for Cu (II)-MIIP and 2.41 mg g^{-1} min^{-1} for MNIP. In addition, no obvious decrease was observed after up to five adsorption cycles, indicating that the Cu (II)-MIIP is of high stability.

1. Introduction

Heavy metals in water have been a major preoccupation for many years because of their toxicity towards aquatic-life, human beings and environment [1]. Heavy metal pollutants are mainly resulted from many industries, such as metal cleaning, mining activities, metal finishing, etc. [2,3]. When these heavy metals are released into the environment, it can cause severe damage to the human body, including accumulative poison, brain damage, and cancer. Therefore, removal of heavy metal ions from wastewater is extremely important.

By far, chemical precipitation [4], ion exchange [5], chitosan [6], natural inorganic mineral [7,8], and functionalized polymers [9] have been employed for the heavy metal removal. Although satisfied results have been achieved by the above methods, major of them need tedious post-processing with secondary pollution and poor reusability. Moreover, all of these methods are applied for non-specific absorption in industry, exhibiting low selectivity. Selective separation of heavy metal ions will facilitate the environment protection and the reuse of precious heavy metal. Therefore, a selective absorption method is required to separate the toxic or precious heavy metal ions from wastewater.

Ionic imprinting technique is one of efficient methods for selectively separating the heavy metal ions. In an ion-imprinting process, the selectivity of a polymeric adsorbent depends on the specificity of the ligand, on the coordination geometry and coordination number of the ions as well as their charges and sizes [10]. Currently, different approaches had been reported for metal ion imprinted polymers, such as bulk polymerization [11], suspension polymerization [12] and precipitation polymerization [13]. However, these conventional methods exhibit some disadvantages, such as low rebinding capacity, slow mass-transfer rate and incomplete removal of templates.

Up to date, surface ion imprinting technique attracted extensive research interest due to complete removal of templates, good accessibility to the target species, low mass-transfer resistance, high adsorption capacity and ease of preparation. Cadmium ion imprinted polymer prepared by Buhani et al. from mercapto-silica through sol–gel process exhibited high selectivity and adsorption capacity towards Cd (II) [14]. Gao et al. [15] prepared surface ionic imprinting materials using surface imprinted technique, and the surface ion imprinting polymer possessed superexcellent binding property and selectivity for template ions. Wang et al. [16] successfully synthesized Pb (II) ion-imprinted mesoporous sorbent by a surface imprinting technique combined with a sol–gel process. The ion-imprinted mesoporous sorbent had been applied to selectively separate and determine Pb (II) in real water samples with satisfactory results. However, very complicated post-processing, such as filter and centrifugal, are required by applying these IIPs. Therefore, it is an urgent need to develop new IIPs which has simple separation process. Furthermore, if IIPs encapsulating Fe_3O_4 as nuclear

* Corresponding author at: Key Laboratory of Jiangxi Province for Ecological Diagnosis-Remediation and Pollution Control, Nanchang 330063, PR China.
Tel.: +86 791 3953372; fax: +86 791 3953373.
E-mail address: luoxubiao@126.com (S. Luo).

0304-3894/$ – see front matter © 2011 Elsevier B.V. All rights reserved.
doi:10.1016/j.jhazmat.2011.05.042

can be synthesized, the magnetic separation will replace the centrifugation and filtration step in a convenient and economical way.

Recently, the preparation of magnetic molecularly imprinted polymers (MMIPs) had been widely reported [17–20]. Few hydroxyl groups existing on the Fe_3O_4 surface result in the difficult graft on Fe_3O_4. If Fe_3O_4 are coated with silica, high graft ratio and high anti-acidic capacity can be obtained on the complex material. Li et al. [17] successfully prepared core–shell MMIPs by the surface RAFT polymerization with the Fe_3O_4 covered with silica serving as core and MIIPs as the shell. The magnetic polymer exhibited good performance, such as good stability under acidic condition, good magnetic property and thermal resistance. To the best of our knowledge, there are few reports on the synthesis of MIIPs by surface ion imprinting technique. Ren et al. [21,22] synthesized magnetic Cu (II)-imprinted composite adsorbent with waste fungal mycelium from industry, chitosan and Fe_3O_4 nanoparticles by embedding method. But it had low selectivity and slow adsorption rate for target ion. In the work, we present a general protocol for synthesizing Cu (II)-MIIP by surface imprinting technique combined with a sol–gel process. The silica layer was modified onto the iron oxide surface by the sol–gel method, and then the complex of Cu (II) and APTES was grafted onto the surface of the Fe_3O_4@SiO_2 particles. The characterization of this MIIP, its adsorption capacity and selectivity were described and discussed in detail.

2. Experimental

2.1. Material

Cupric chloride, zinc chloride, nickel sulfate hex hydrate, tetraethyl orthosilicate (TEOS), 2-propanol, ammonia solution (28%) and 3-aminopropyltriethoxysilane (APTES) were supplied by Pure Crystal Shanghai Reagent Co., Ltd. (Shanghai, China). Ferric chloride ($FeCl_3{\cdot}6H_2O$) and ferrous sulfate ($FeSO_4{\cdot}7H_2O$) were obtained from Shenyang Chemical Industry Corporation (Shenyang, China). Water was purified through a Milli-Q water system (Bedford, USA). All other chemicals were of analytical reagent grade.

2.2. Preparation of Fe_3O_4@SiO_2

The Fe_3O_4 magnetic nanoparticles were prepared according to Ref. [23]. Fe_3O_4@SiO_2 microspheres were prepared according to the method with minor modification [24]. Typically, 5.00 g magnetite nanoparticles were dissolved in 250 mL 2-propyl alcohol and 20 mL highly purified water by sonication for 15 min, followed by the addition of 20 mL ammonia solution and 33.3 mL TEOS sequentially. The resultant product was collected by an external magnetic field after 12 h duration time at the room temperature under a continuous stirring, and rinsed with highly purified water for five times thoroughly.

2.3. Preparation of Fe_3O_4@SiO_2-IIP and Fe_3O_4@SiO_2-NIP

Firstly, 0.75 g $CuCl_2$ and 60 mL methanol were mixed and heated by the water bath. Then, 4 mL APTES was added into the previous mixture. Finally, the reaction mixture was stirred and refluxed for 1 h.

Secondly, 5 g of Fe_3O_4@SiO_2 suspended solution was quickly stirred to achieve uniform distribution of Fe_3O_4@SiO_2 particles. Then, 50 mL of Fe_3O_4@SiO_2–methanol suspended solution was added into the above solution. The reaction mixture was stirred and refluxed for 24 h.

Thirdly, the reaction products were separated by magnet and washed by methanol for three times. Afterward, particles were fully washed with 2 M hydrochloric acid solution to remove the Cu (II) (this step was repeated three times), followed by washing with extensive distilled water until the washing water was neutral. Finally, the Fe_3O_4@SiO_2-IIP was obtained under an external magnetic field.

The synthesis route of Fe_3O_4@SiO_2-MIIP is given in Fig. 1. Fe_3O_4@SiO_2-NIP was prepared with the same procedures as above described without adding $CuCl_2$.

2.4. Characterization

Fourier transform infrared (FT-IR) spectra were recorded on a Varian scimitar 2000 (Varian Corp., USA). Magnetic characteristics of Fe_3O_4 and Cu (II)-MIIP were measured with a LakeShore

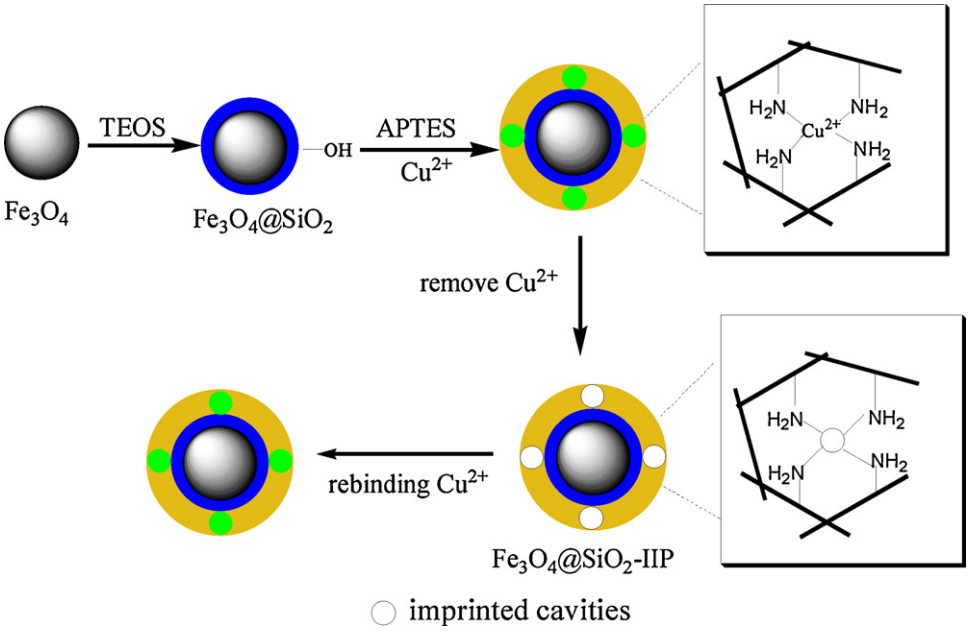

Fig. 1. Synthesis route of Fe_3O_4@SiO_2-IIP.

7307 (America, LDJ9600) VSM at 300 K. XRD measurement was performed using a monochromatized X-ray beam with nickel-filtered Cu Kα radiation (λ = 0.1542 nm). A continuous scan mode was applied to collect 2θ data from 20° to 80° (Japan, Shimadzu).

The adsorption capacities of Fe_3O_4@SiO_2-IIP and Fe_3O_4@SiO_2-NIP were determined by flame atomic absorption spectrometer (Purkinje General, China).

2.5. Static adsorption experiments

The pH effect on the adsorption of Cu (II) ions was tested by mixing 50 mg Fe_3O_4@SiO_2-IIP and 50 mL of 80 mg/L Cu (II) at various pH values for 20 min. The pH of solution was adjusted using hydrochloric acid or sodium hydroxide.

The IIP and NIP adsorption studies for the Cu (II) ions were carried out batch experiments. In order to determine the Fe_3O_4@SiO_2-IIP adsorption capacity, 50 mg Fe_3O_4@SiO_2-IIP and Fe_3O_4@SiO_2-NIP were introduced into different glass flasks, respectively. 50 mL of Cu (II) solution with initial concentration c_0 (20 mg/L, 30 mg/L, 40 mg/L, 50 mg/L, 60 mg/L, 70 mg/L, 80 mg/L, and 100 mg/L) were then added into each glass flask. The flasks contained those mixture solution were shaken for 20 min. Then the adsorbent was separated from the liquid solution by external magnet and the concentration of Cu (II) ions in the remaining solutions was determined by flame atom absorption spectrophotometer. The equilibrium binding amounts of Fe_3O_4@SiO_2-IIP towards Cu (II) ions was calculated according to Eq. (1), and the binding isotherm was plotted.

$$Q_e = \frac{V(c_0 - c_e)}{m} \quad (1)$$

where c_0 (mg/L) is the initial concentration of Cu (II) ions (without absorbent) and c_e is the equilibrium concentration of Cu (II) ions; V (L) is the volume of the Cu (II) solution; m is the mass of the Fe_3O_4@SiO_2-IIP; Q_e (mg/g) is the equilibrium binding quantity of Fe_3O_4@SiO_2-IIP for Cu (II) ions.

Similarly, binding isotherm of Fe_3O_4@SiO_2-NIP for Cu (II) ions was measured using the similar procedures of Fe_3O_4@SiO_2-IIP for Cu (II) ions.

2.6. Dynamic binding characters of Fe_3O_4@SiO_2-IIP towards template

At room temperature, 50 mL Cu (II) solution with a concentration of 80 mg/L was loaded into a conical flask. 50 mg Fe_3O_4@SiO_2-IIP particles were added into the flask, and the solution was shaken on a constant temperature shaker. After an interval of time, the mixture was taken out and separated under an external magnetic field, and the Cu (II) concentration in the supernatant was determined with flame atom absorption spectrophotometer. The time in which the adsorption reached to equilibrium was determined.

$$Q = \frac{V(c_0 - c_t)}{m} \quad (2)$$

Where c_0 (mg/L) is the initial concentration of Cu (II) (without absorbent) and c_t is the concentration of Cu (II) ions at any time t, V (L) is the volume of the Cu (II) solution; m is the mass of the Fe_3O_4@SiO_2-IIP; Q(mg/g) is the binding quantity of Fe_3O_4@SiO_2-IIP for Cu (II) ions.

The dynamic binding property of Fe_3O_4@SiO_2-NIP towards Cu (II) ions was measured as the same as method.

2.7. Selectivity experiments

The competitive absorption experiments were conducted by preparing mixture of Cu (II), Zn (II) and Ni (II), and each metal ion initial concentration was 80 mg/L. In order to investigate the selectivity of the adsorbent, static adsorption experiment results were used for evaluation. Distribution coefficient was calculated by Eq. (3), and this equation was derived from the equation of Ref. [25]:

$$K_d = \frac{C_p}{C_e} \quad (3)$$

where K_d is the distribution coefficient; C_e is the equilibrium concentration of Cu (II) ions; C_p is the amount of Cu (II) adsorbed on per weight unit of solid after equilibrium. The selectivity coefficient for the binding of Cu (II) ions in the presence of competitor ions can be obtained from equilibrium binding data according to Eq. (4):

$$K = \frac{K_d\ (\mathrm{Cu\,(II)})}{K_d\,(\mathrm{M\,(II)})} \quad (4)$$

where K is the selectivity coefficient, M (II) represents Zn (II) or Ni (II). K represents Cu (II) adsorption selectivity when there are other metal ions in aqueous solution. The larger K indicates a stronger choice ability for the Cu (II).

$$K' = \frac{K_{\mathrm{imprinted}}}{K_{\mathrm{non\text{-}imprinted}}} \quad (5)$$

A relative selectivity coefficient, K', can be defined by Eq. (5) and the larger of K' can indicate the enhanced extent of adsorption affinity and selectivity of magnetic imprinting material for the template with respect to non-imprinting material.

3. Results and discussion

3.1. Characterization of the Fe_3O_4@SiO_2-IIP

3.1.1. FTIR analysis

FT-IR is employed to characterize Fe_3O_4 (A), Fe_3O_4@SiO_2 (B), Fe_3O_4@SiO_2-IIP (C), and Fe_3O_4@SiO_2-NIP (D). As shown in Fig. 2, the bands at 571 cm^{-1} are indicative to the presence of the Fe–O–Fe bond. The absorption around 960 cm^{-1} and 1080 cm^{-1} indicate Si–O–H and Si–O–Si stretching vibrations. The presence of adsorption water is reflected by –OH vibration at 1630 and 3440 cm^{-1}. Moreover, Fe_3O_4@SiO_2 of –OH vibration intensity are far greater than the Fe_3O_4, which suggests that SiO_2 has been successfully

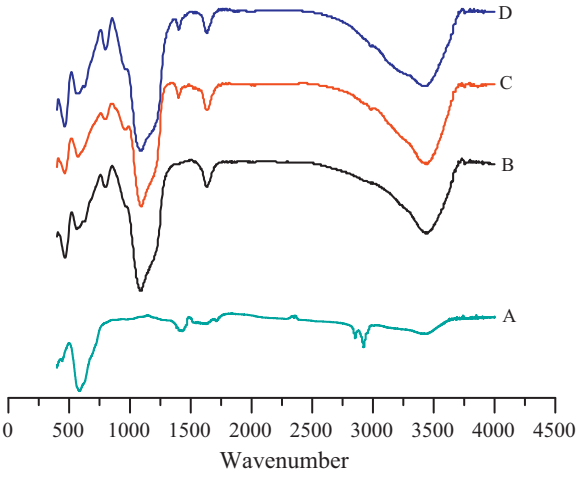

Fig. 2. Infrared spectra of Fe_3O_4 (A), Fe_3O_4@SiO_2 (B), Fe_3O_4@SiO_2-IIP (C), and Fe_3O_4@SiO_2-NIP (D).

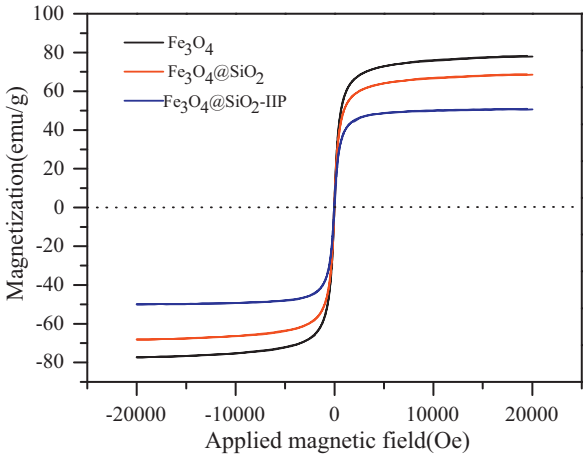

Fig. 3. Magnetization curve of pure Fe_3O_4 particles (*S* saturation magnetization is 77.90 emu/g) Fe_3O_4@SiO_2 (*S* saturation magnetization is 68.50 emu/g), Fe_3O_4@SiO_2-IIP (*S* saturation magnetization is 50.60 emu/g).

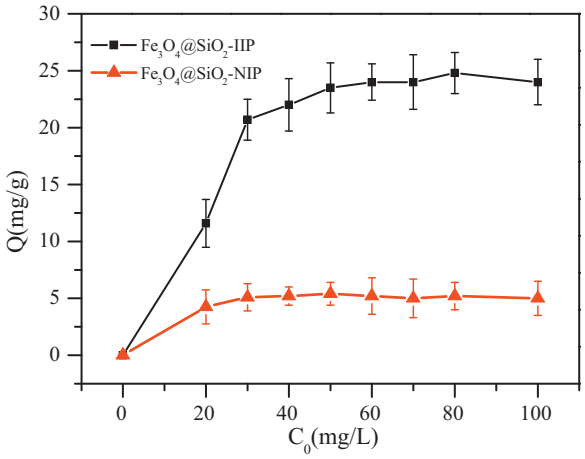

Fig. 5. Cu (II) adsorption isotherms for Fe_3O_4@SiO_2-IIP and Fe_3O_4@SiO_2-NIP. Conditions: sorbents 50 mg, shaking time 20 min, temperature 25 °C.

immobilized on Fe_3O_4 surface. After grafting of the amino functionality, a very weak N–H stretching peak can be seen at 1396 cm^{-1} for Fe_3O_4@SiO_2-IIP and Fe_3O_4@SiO_2-NIP. The result indicates that APTES has been successfully immobilized on Fe_3O_4@SiO_2 surface, and both Fe_3O_4@SiO_2-IIP and Fe_3O_4@SiO_2-NIP possess similar component.

3.1.2. Magnetism analysis

The magnetic hysteresis loops of Fe_3O_4, Fe_3O_4@SiO_2 and Fe_3O_4@SiO_2-IIP are illustrated in Fig. 3. The magnetic hysteresis loops of three samples all through the origin, indicating a paramagnetic material. The Fe_3O_4, Fe_3O_4@SiO_2 and Fe_3O_4@SiO_2-IIP achieved a saturation magnetization value(s) is 77.90, 68.50 and 50.60 emu/g, respectively. The slight decrease of saturation magnetic intensity can also indicate the layer of APTES polymer on the surface of Fe_3O_4@SiO_2 is very thin, which resulted in less diffusion barrier to template ion, and easily reached the magnetic separation under an external magnetic field.

3.1.3. XRD analysis

As can be seen in Fig. 4, six characteristic peaks of Fe_3O_4 (2θ = 30.1, 35.4, 43.0, 53.5, 57.0 and 62.5) are observed. This six peaks corresponding to the six crystal faces are (2 2 0), (3 1 1), (4 0 0), (4 2 2), (5 1 1), and (4 4 0), respectively. These peaks are consistent with the database in MDI Jade 5.0X analyse software. The results indicate that the resultant particles are Fe_3O_4 with a spinel

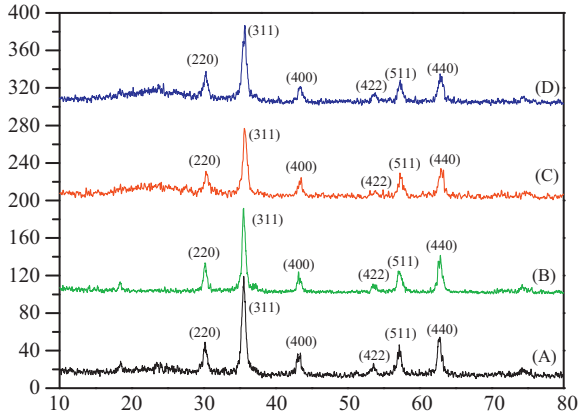

Fig. 4. XRD patterns of Fe_3O_4 (A), Fe_3O_4@SiO_2 (B), Fe_3O_4@SiO_2-IIP (C), and Fe_3O_4@SiO_2-NIP (D).

structure. The six peaks of the Fe_3O_4 in Fig. 5(B) could be seen for the synthesized Fe_3O_4@SiO_2 but the intensity slightly decreases, the result suggests that SiO_2 has been successfully wrapped onto the surface of Fe_3O_4. The six peaks of the Fe_3O_4 in Fig. 5(C) and (D) could be seen for the synthesized Fe_3O_4@SiO_2-IIP and Fe_3O_4@SiO_2-NIP but the intensity slightly decrease. Moreover, the peak positions are unchanged upon coating of SiO_2 and polymerization, indicating that the crystalline structure of the magnetite is essentially maintained. This is in agreement with the results reported in the literature [26,27]. These results may indicate that APTES is immobilized on the surface of Fe_3O_4 successfully.

3.2. Absorption experiment

3.2.1. Absorption capacity

Fig. 5 shows the concentration effect on the adsorption capacity for the Cu (II) ions. When the Cu (II) concentration increase, the adsorption amount firstly increases sharply, then increase slightly, and finally, reach saturation. The maximum absorption capacities are 24.20 and 5.20 mg/g for Fe_3O_4@SiO_2-IIP and Fe_3O_4@SiO_2-NIP, respectively. The absorption capacity of Fe_3O_4@SiO_2-IIP is enhanced almost 4.65 times than that of Fe_3O_4@SiO_2-NIP, displaying the excellent recognition selectivity and binding affinity towards Cu (II) ions in aqueous solution.

The equilibrium adsorption data were fitted, according to the Langmuir model as shown by the following equations: (Eq. (6))

$$\text{Langmuir model}: \frac{C_e}{Q} = \frac{C_e}{Q_{max}} + \frac{1}{bQ_{max}} \quad (6)$$

where C_e is the equilibrium of final concentration of Cu (II) ions in solution, Q is the adsorption capacity of Cu (II) ions adsorbed on the Fe_3O_4@SiO_2-IIP at equilibrium concentration, Q_{max} is the maximum adsorption capacity, and b is the Langmuir constant.

Linear plots of C_e/Q versus C_e were employed to determine the value of Q_{max} and b. The regress data fitted the equations are shown in Fig. 6. The Langmuir constants are summarized in Table 1. The data obtained with correlation coefficients (R^2) of Fe_3O_4@SiO_2-IIP and Fe_3O_4@SiO_2-NIP are 0.9900 and 0.9960,

Table 1
Langmuir adsorption isotherm constants for Cu (II) on Fe_3O_4@SiO_2-IIP and Fe_3O_4@SiO_2-NIP.

Adsorbents	Q_{max} (mg/g)	b (L/mg)	R^2
Fe_3O_4@SiO_2-IIP	26.25	0.21	0.9900
Fe_3O_4@SiO_2-NIP	5.13	3.25	0.9960

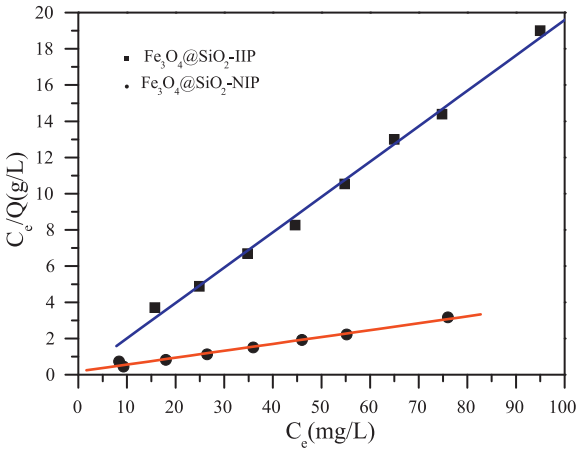

Fig. 6. Langmuir plot for the adsorption of Cu (II) on Fe_3O_4@SiO_2-IIP and Fe_3O_4@SiO_2-NIP.

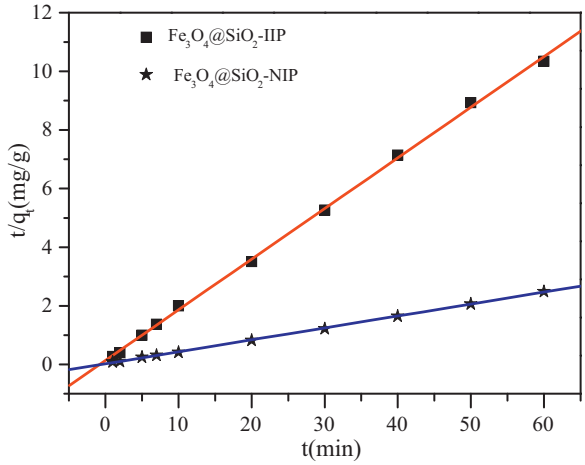

Fig. 8. Linear plot of t/q_t vs. t for Fe_3O_4@SiO_2-IIP and Fe_3O_4@SiO_2-NIP.

respectively. The experimental values of Q_e are 24.20 and 5.20 mg/g for Fe_3O_4@SiO_2-IIP and Fe_3O_4@SiO_2-NIP, respectively. It is very close to the calculated Q_{max} value, which showed that all the sorption sites were almost homogeneous.

3.2.2. Adsorption kinetics

Fig. 7 shows adsorption of Cu (II) on Fe_3O_4@SiO_2-IIP and Fe_3O_4@SiO_2-NIP sorbent from aqueous solution containing 80 mg/L of Cu (II) with various contact times. Obviously, Fe_3O_4@SiO_2-IIP and Fe_3O_4@SiO_2-NIP show a good performance in adsorption during the first 2 min. The time required to achieve the adsorption equilibrium is only 10 min, and there is no obvious change from 10 to 60 min. So, the Fe_3O_4@SiO_2-IIP and Fe_3O_4@SiO_2-NIP can achieve adsorptive equilibrium in a relative short time for Cu (II) ions. The results suggest the Fe_3O_4@SiO_2-IIP has small mass-transfer resistance.

To investigate the controlling mechanism of adsorption processes such as mass transfer and chemical reaction, the kinetic data obtained from batch experiments were fitted pseudo-second-order rate equation. Assuming that the adsorption capacity of adsorbent is proportional to the number of active sites on its surface, it was developed by Ho and McKay [28] as Eq. (7):

$$\frac{t}{q_t} = \frac{1}{k_2 q_e^2} + \frac{1}{q_e} t \tag{7}$$

where q_e and q_t are the amounts of Cu (II) ions adsorbed onto adsorbent at equilibrium and any time t, respectively (mg/g) and k_2 is the second-order rate constant at the equilibrium (mg g^{-1} min^{-1}), $h_0 = k_2 q_e^2$ is the initial adsorption rate (mg g^{-1} min^{-1}). The regress data fitted the equation is shown in Fig. 8. The adsorption kinetic constants and linear regression values are summarized in Table 2. The data obtained with correlation coefficients (R^2) of Fe_3O_4@SiO_2-IIP and Fe_3O_4@SiO_2-NIP are 0.9992 and 0.9996, respectively. The theoretical q_e value estimated from the pseudo-second-order kinetic model is also very close to the experimental value. These results suggest that the pseudo-second-order mechanism is predominant and that chemisorption may be the rate-limiting step that controls the adsorption process.

Table 2
Kinetic parameters of the pseudo-second-order rate equation for Cu (II) adsorption on Fe_3O_4@SiO_2-IIP and Fe_3O_4@SiO_2-NIP.

Sorbents	k_2	q_e	h_0	R^2
Fe_3O_4@SiO_2-IIP	0.22	24.54	132.48	0.9992
Fe_3O_4@SiO_2-NIP	0.072	5.79	2.41	0.9996

3.2.3. Effect of pH

The pH is one of the most important parameters controlling the metal ion adsorption process. The pH effect on adsorption capacity for Cu (II) ions is shown in Fig. 9. The adsorption capacity of Cu (II) increases as the pH of the aqueous solution increased from 2 to 5. The maximum adsorption capacity is observed when the pH increases to pH = 5. Below pH 3, the Fe_3O_4@SiO_2-IIP of adsorptive

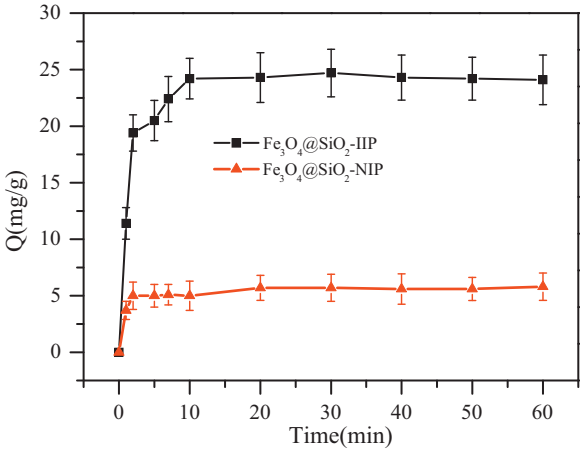

Fig. 7. Effect of equilibrium time on adsorption of Fe_3O_4@SiO_2-IIP and Fe_3O_4@SiO_2-NIP Conditions: sorbents 50 mg, concentration 80 mg/L, temperature 25 °C.

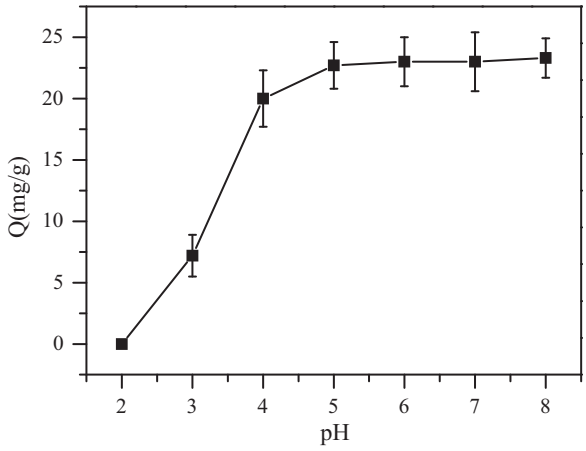

Fig. 9. Effect of pH on the adsorption capacity of Fe_3O_4@SiO_2-IIP.

Table 3
Adsorption selectivity of Fe_3O_4@SiO_2-IIP and Fe_3O_4@SiO_2-NIP.

Metal ions	Fe_3O_4@SiO_2-IIP			Fe_3O_4@SiO_2-NIP	
	K_d	K	K_d	K	K'
Cu (II)	450.00		69.50		
Zn (II)	4.90	91.84	22.04	3.15	29.16
Ni (II)	3.36	133.92	19.82	3.51	38.15

capacity is very low. This is mainly due to the protonation of the amine moiety, which diminished the chelate ability of the amino group with the Cu (II) ions in aqueous solution.

3.2.4. Selectivity experiments

Zn (II) and Ni (II) are chosen as the competitor ions, due to the same charge, nearly identical size (ionic radius: Zn (II), 74 pm; Ni (II), 72 pm; and Cu (II), 69 pm). From the data in Table 3, the following facts can be found: (1) the distribution coefficient of Fe_3O_4@SiO_2-IIP for Cu (II) is far greater than Zn (II), Ni (II); (2) the selectivity coefficients of Fe_3O_4@SiO_2-NIP is far lower than Fe_3O_4@SiO_2-IIP, the low selectivity coefficients of Fe_3O_4@SiO_2-NIP for the three ions are only caused by different chelation forces between N atoms of APTES and metal ions; (3) the relative selectivity coefficient is an indication of the relative adsorption affinity of the imprinted ions. The relative selectivity coefficients of Fe_3O_4@SiO_2-IIP for Cu (II)/Zn (II) and Cu (II)/Ni (II) were 29.16 and 38.15 times higher than those of Fe_3O_4@SiO_2-NIP, respectively. The above results suggest the binding abilities of Fe_3O_4@SiO_2-IIP for Cu (II) is stronger than that for Zn (II) and Ni (II). Although all the chelates of the three ions with APTES are of four ligands, the binding abilities of Fe_3O_4@SiO_2-IIP for Zn (II) and Ni (II) are very poor. The reason for this is that the cavities imprinted by Cu (II) are not suited to Zn (II) and Ni (II) in size, shape and spatial arrangement of action sites. The ionic radius of both Zn (II) (74 pm) and Ni (II) (72 pm) are larger than that of Cu (II) (69 pm).

3.3. Application of Fe_3O_4@SiO_2-IIP

The prepared Fe_3O_4@SiO_2-IIP was applied for the removal of Cu (II) ions from river water (Ganjiang River, Nanchang). The rive water was spiked 20 mg/L of Cu (II) ions. The spiked river water was treated according to the optimal experimental conditions. The Fe_3O_4@SiO_2-IIP exhibits almost 100% removal efficiencies, suggesting that Fe_3O_4@SiO_2-IIP has a strong anti-interference ability in real water samples.

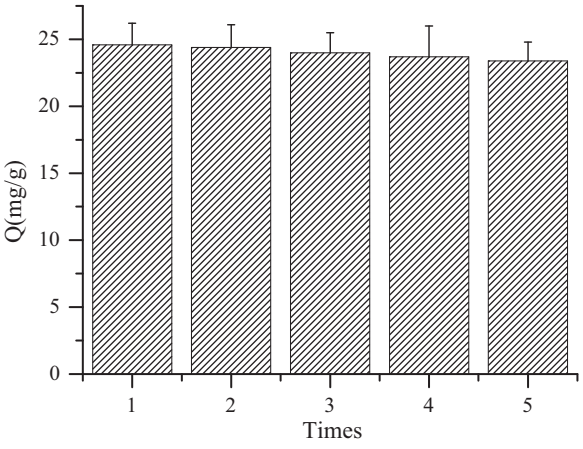

Fig. 10. Reusability of Fe_3O_4@SiO_2-IIP. Conditions: sorbents 50 mg, concentration 80 mg/L, shaking time 20 min, temperature 25 °C.

3.4. Reusability

The stability and potential regeneration of the Fe_3O_4@SiO_2-IIP were investigated. The regeneration of the Fe_3O_4@SiO_2-IIP was dipped in 20 mL 2 M hydrochloric acid for 15 min and concentrated ammonia solution for 5 min, respectively. Adsorption results of repeated uses in Fe_3O_4@SiO_2-IIP are shown in Fig. 10. The Fe_3O_4@SiO_2-IIP can be reused after extraction with hydrochloric acid, and is stable for up to five adsorption cycles without obvious decrease in the adsorption capacity for Cu (II). The results suggest that the Fe_3O_4@SiO_2-IIP have certain regeneration adsorption efficiency, and could be used repeatedly.

4. Conclusions

In this work, a novel Fe_3O_4@SiO_2-IIP sorbent was successfully prepared by combining a surface ion imprinting technique with a sol–gel process. The Fe_3O_4@SiO_2-IIP had high chemical stability, excellent reproducibility, good magnetic property, fast adsorption kinetics and strong acid resistance. The obtained Fe_3O_4@SiO_2-IIP exhibited a very high degree of selectivity and adsorption ability towards the Cu (II) ions. The new surface magnetic ion imprinted polymers might be providing a reliable and effective solution to recover and utilize precious heavy metal from industrial wastewater.

Acknowledgements

This work was financially supported by a grant from National Science Fund for Distinguished Young Scholars (50725825), National Natural Science Foundation of China (50978132), Natural Science Foundation of Jiangxi Province of China (2009GQH0083), and Science and Technology Supported Program of Jiangxi Province of China (2009BSB09800).

References

[1] A. Stafiej, K. Pyrzynska, Adsorption of heavy metal ions with carbon nanotubes, Sep. Purif. Technol. 58 (2007) 49–52.
[2] B.G. Wei, L.S. Yang, A review of heavy metal contaminations in urban soils, urban road dusts and agricultural soils from China, Microchem. J. 94 (2010) 99–107.
[3] F.L. Fu, Q. Wang, Removal of heavy metal ions from wastewaters: a review, J. Environ. Manage. 92 (2011) 407–418.
[4] J.S. Espana, E.L. Pamo, E.S. Pastor, J.R. Andres, J.A.M. Rubi, The removal of dissolved metals by hydroxysulphate precipitates during oxidation and neutralization of acid mine waters, Aquat. Geochem. 12 (2006) 269–298.
[5] M.G. Fonseca, M.M. Oliveora, L.N.H. Arakaki, J.G.P. Espinola, C. Airoldi, Natural vermiculite as an exchanger support for heavy cat in aqueous, J. Colloid Interface Sci. 285 (2005) 50–55.
[6] A.H. Chen, S.C. Liu, C.Y. Chen, C.Y. Chen., Comparative adsorption of Cu (II) Zn (II), and Pb (II) in aqueous solution on the crosslinked chitosan with epichlorohydrin, J. Hazard. Mater. 154 (2008) 184–191.
[7] M. Dogan, A. Turkyilmaz, M. Alkan, O. Demirbas, Adsorption of copper (II) onto sepiolite and electrokinetic properties, Desalination 238 (2009) 257–270.
[8] M. Yavus, F. Gode, E. Phelivan, S. Ozmert, Y.C. Sharma, An economic removal of Cu^{2+} and Cr^{2+} on the new adsorbents: pumice and polyacrylonitrile/pumice composite, Chem. Eng. J. 137 (2008) 453–461.
[9] L.C. Zhou, Y.F. Li, X. Bai, G.H. Zhao, Use of microorganisms immobilized on composite polyurethane foam to remove Cu (II) from aqueous solution, J. Hazard. Mater. 167 (2009) 1106–1113.
[10] M. Andac, E. Özyapı, S. Senel, R. Say, A. Denizli, Ion-selective imprinted beads for aluminum removal from aqueous solutions, Ind. Eng. Chem. Res. 45 (2006) 1780–1786.
[11] C. Esen, M. Andac, N. Bereli, R. Say, E. Henden, A. Denizli, Highly selective ion-imprinted particles for solid-phase extraction of Pb^{2+} ions, Mater. Sci. Eng. C 29 (2009) 2464–2470.
[12] N.T. Hoai, D.K. Yoo, D. Kim, Batch and column separation characteristics of copper-imprinted porous polymer micro-beads synthesized by a direct imprinting method, J. Hazard. Mater. 173 (2010) 462–467.
[13] J. Otero-Romaní, A. Moreda-Piñeiroa, P. Bermejo-Barrera, A. Martin-Esteban, Synthesis, characterization and evaluation of ionic-imprinted polymers for solid-phase extraction of nickel from seawater, Anal. Chim. Acta 630 (2008) 1–9.

[14] Buhani, Narsito, Nuryono, E.S. Kunarti, Production of metal ion imprinted polymer from mercapto-silica through sol–gel process as selective adsorbent of cadmium, Desalination 251 (2010) 83–89.
[15] B.J. Gao, F.Q. An, Y. Zhu, Novel surface ionic imprinting materials prepared via couple grafting of polymer and ionic imprinting on surfaces of silica gel particles, Polymer 48 (2007) 2288–2297.
[16] L.M. Wang, M.H. Zhou, Z.J. Jing, A. Zhong, Selective separation of lead from aqueous solution with a novel Pb (II) surface ion-imprinted sol–gel sorbent, Microchim. Acta 165 (2009) 367–372.
[17] Y. Li, X. Li, J. Chu, C. Dong., Synthesis of core–shell magnetic molecular imprinted polymer by the surface RAFT polymerization for the fast and selective removal of endocrine disrupting chemicals from aqueous solutions, Environ. Pollut. 158 (2010) 2317–2323.
[18] Y. Zhang, R. Liu, Y. Hu, G. Li, Microwave heating in preparation of mag-MIP beads for trace triazines analysis in complicated sample, Anal. Chem. 81 (2009) 967–976.
[19] C.J. Tan, H.G. Chua, K.H. Ker, Y.W. Tong., Preparation of bovine serum albumin surface-imprinted submicrometer particles with magnetic susceptibility through core shell miniemulsion polymerization, Anal. Chem. 80 (2008) 683–692.
[20] L.G. Chen, J. Liu, Q.L. Zeng, H. Wang, A. Yu, H. Zhang, L. Ding., Preparation of magnetic molecularly imprinted polymer for the separation of tetracycline antibiotics from egg and tissue samples, J. Chromatogr. A 1216 (2009) 3710–3719.
[21] Y.M. Ren, M.L. Zhang, D. Zhao., Synthesis and properties of magnetic Cu (II) ion imprinted composite adsorbent for selective removal of copper, Desalination 228 (2008) 135–149.
[22] Y.M. Ren, X.Z. Wei, M.L. Zhang, Adsorption character for removal Cu (II) by magnetic Cu (II) ion imprinted composite adsorbent, J. Hazard. Mater. 158 (2008) 14–22.
[23] X.B. Wang, X.B. Ding, Z.H. Zheng, Magnetic molecularly imprinted polymer particles synthesized by suspension polymerization in silicone oil, Macromol. Rapid Commun. 27 (2006) 1180–1184.
[24] X. Wang, L.Y. Wang, X.W. He, Y.K. Zhang, L.X. Chen., A molecularly imprinted polymer-coated nanocomposite of magnetic nanoparticles for estrone recognition, Talanta 78 (2009) 327–332.
[25] E. Birlik, A. Ersoz, E. Acykkalp, A. Denizli, R. Say, Cr (III)-imprinted polymeric beads: sorption and preconcentration studies, J. Hazard. Mater. B140 (2007) 110–116.
[26] G.Y. Li, K.L. Huang, Preparation and characterization of *Saccharomyces cerevisiae* alcoholdehydrogenase immobilized on magnetic nanoparticles, Int. J. Biol. Macromol. 42 (2008) 405–412.
[27] A. Zhu., Suspension of Fe_3O_4 nanoparticles stabilized by chitosan and o-carboxymethylchitosan, Int. J. Pharm. 350 (2008) 361–368.
[28] Y.S. Ho, G. McKay, Kinetic models for the sorption of dye from aqueous solution by wood, Trans. Inst. Chem. Eng. 76B (1998) 183–191.